

Preparation of Poly(methyl methacrylate)/Na-MMT Nanocomposites via *in-Situ* Polymerization with Macroazoinitiator

Han Mo Jeong* and Young Tae Ahn

Research Center for Machine Parts and Materials Processing, Department of Chemistry,
University of Ulsan, Ulsan 680-749, Korea

Received October 13, 2004; Revised February 25, 2005

Abstract: Poly(methyl methacrylate) (PMMA)/sodium montmorillonite (Na-MMT) nanocomposites were prepared with a novel method utilizing a macroazoinitiator (MAI). To induce the intergallery polymerization of methyl methacrylate (MMA), the MAI containing a poly(ethylene glycol) (PEG) segment was intercalated between the lamellae of Na-MMT and swelled with water to enhance the diffusion of MMA into the gallery. The structure of the nanocomposite was examined using X-ray diffraction and transmission electron microscopy, and the thermal properties were examined using differential scanning calorimetry and thermogravimetry. The PMMA/Na-MMT nanocomposite prepared by intergallery polymerization showed a distinct enhancement of its thermal properties; an approximately 30 °C increase in its glass transition temperature and an 80–100 °C increase in its thermal decomposition temperature for a 10% weight loss.

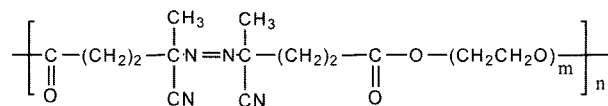
Keywords: poly(methyl methacrylate), sodium montmorillonite, nanocomposite, macroazoinitiator, exfoliation.

Introduction

In recent years, polymer/silicate nanocomposites have attracted considerable attention as advanced materials, because many physical properties of matrix polymers such as their mechanical, barrier and flame-retarding properties can be substantially enhanced with small amounts of silicate compared to conventional composites.¹⁻⁴ Because these unique properties of polymer/silicate nanocomposites come from their high surface-to-volume ratio of fillers, layered silicates such as montmorillonite, which are composed of stacks of parallel lamellae with a 1 nm thickness and a high aspect ratio, are most commonly utilized as a filler.⁵

In-situ polymerization of monomer in the presence of layered silicate is a widely-used method to prepare nanocomposites.⁶⁻¹² When the polymerization occurs at the gallery between the parallel lamellae of silicate, we can anticipate that the layers will be pushed apart and eventually delaminate to give an exfoliated nanocomposite. So, the intergallery polymerization via a silicate-anchored initiator has been reported by some researchers as an effective method to make nanocomposites.¹³⁻¹⁶ In these researches, initiators were designed to have cationic sites which can adhere to silicates by an ionic interaction.

As a new approach, we used a physically intercalated macroazoinitiator (MAI) with the following chemical structure in this study to induce the intergallery polymerization of methyl methacrylate (MMA). The MAI was designed to have a poly(ethylene glycol) (PEG) segment, because PEG blocks can be easily intercalated between the gallery of sodium montmorillonite (Na-MMT). The intercalated PEG/Na-MMT compound has high stability that PEG cannot be replaced by organic compounds having high affinity toward Na-MMT, such as dimethyl sulfoxide and crown ethers.^{17,18}



Most researchers have used organically-modified Na-MMT to prepare the nanocomposite of poly(methyl methacrylate) (PMMA).^{19,20} Some researchers have reported that PMMA/pristine Na-MMT nanocomposite can be effectively prepared by suspension or emulsion polymerization.^{13,21}

In this study, a new system, water-swelled MAI/Na-MMT compounds, was used to prepare the PMMA/Na-MMT nanocomposite with an exfoliated structure via *in-situ* polymerization. The structure, the thermal properties, and the stability of these nanocomposites were examined.

*e-mail: hmjeong@mail.ulsan.ac.kr

1598-5032/04/102-05 © 2005 Polymer Society of Korea

Experimental

Na-MMT (Southern Clay) was used after drying at 60 °C in a vacuum for 2 days. MAI (Wako Pure Chemical, VPE-0201) was used as received. It was the condensation polymer of 4,4'-azobis(4-cyanopentanoic acid) and PEG whose molecular weight was 2,000.²² Its molecular weight was about 22,000 and its azo group content was 0.45 mmol/g. MMA (Aldrich) was purified by usual procedures.²³ 2,2'-Azobisisobutyronitrile (AIBN, Aldrich), acetonitrile (Aldrich), and methanol (Aldrich) were used as received.

MAI intercalated Na-MMT (MAI/Na-MMT nanocomposite) was prepared using an acetonitrile/methanol mixture (1/1 by volume) as a solvent.^{17,18} That is, 3 g of MAI was dissolved in 100 mL of solvent and they were stirred with 7 g of Na-MMT for 1 day at room temperature. The intercalated compound was separated with a centrifuge, and repeatedly washed with acetonitrile and methanol to remove nonintercalated physisorbed MAI.¹⁷ It was dried at 25 °C for 48 hrs in a vacuum before use.

The recipes for the preparation PMMA/Na-MMT nanocomposites are shown in Table I. In the cases of Series I and Series II, initiators, AIBN and MAI were dissolved in MMA, and the bulk radical copolymerization of MMA in the presence of Na-MMT was carried out by stirring with a magnetic bar at 60 °C under N₂ atmosphere for 48 hrs. In the case of Series III, MAI/Na-MMT nanocomposite was swelled in a reactor with 10-fold of water, then MMA was fed dropwisely into the reactor being stirred by a magnetic bar at room temperature. After the feeding of MMA, this heterogeneous system was heated to 60 °C and polymerization was

carried out at 60 °C under N₂ atmosphere for 48 hrs. The prepared PMMA/Na-MMT nanocomposites were crushed into powder and dried at 100 °C for 12 hrs in a vacuum to remove low molecular weight components.

X-ray diffraction (XRD) patterns were obtained with an X-ray diffractometer (XPERT, Philips) using Cu K_α radiation (=1.54 Å) as the X-ray source. The diffraction angle was scanned from 1.2° at a rate of 1.2°/min.

The morphology of nanocomposites was examined with a transmission electron microscope (TEM, Hitachi H-8100). Thin sections were cut perpendicular to the flow direction of nanocomposite fiber, which was extruded by a melt indexer at 230 °C. The accelerating voltage of TEM was 200 kV.

Differential scanning calorimetry (DSC) was carried out with DSC-2910 (TA Instruments) at a heating and cooling rate of 10 °C/min with a 5 mg sample. The nanocomposite stayed at 150 °C for 5 min in DSC, and was cooled down to 25 °C. The glass transition temperature (*T_g*) was determined in the subsequent heating scan.

Thermogravimetric analysis (TGA) was carried out with a thermogravimetric analyzer (TA Instruments, TGA 2950) at a heating rate of 10 °C/min under N₂ atmosphere with a sample of 30 mg in a platinum crucible.

Results and Discussion

Figure 1(a) and 1(b) show the XRD patterns of Na-MMT and MAI/Na-MMT nanocomposite. We can see that Na-MMT and MAI/Na-MMT nanocomposite have a peak at $2\theta = 7.9^\circ$ and $2\theta = 5.0^\circ$, respectively. This shows that the gallery height calculated by Bragg's law, $d = \lambda/2 \sin \theta$, was

Table I. Recipe for the Preparation of PMMA/Na-MMT Nanocomposite and Polymerization Yield

Designation Code	Feed						Polymerization Yield (%)
	MMA (wt %)	AIBN (wt %)	MAI (wt %)	Na-MMT (wt %)	MAI/Na-MMT (wt %)	Concentration of Azo Group (mmol/100g-MMA)	
<i>Series I</i>							
C00E0	99.70	0.30	-	-	-	1.80	90.9
C03E0	96.80	0.29	-	2.91	-	1.79	89.9
C05E0	94.98	0.29	-	4.74	-	1.81	87.9
C07E0	93.20	0.28	-	6.53	-	1.80	80.1
<i>Series II</i>							
C03E06	96.24	0.24	0.63	2.89	-	1.80	89.0
C05E10	94.06	0.21	1.03	4.71	-	1.80	89.6
C07E14	91.98	0.17	1.41	6.44	-	1.80	86.4
<i>Series III</i>							
C03E06W	96.47	-	-	-	0.64/2.89	0.30	83.4
C05E10W	94.26	-	-	-	1.05/4.70	0.50	82.2
C07E14W	92.14	-	-	-	1.43/6.43	0.70	83.4
C10E20W	89.13	-	-	-	1.98/8.90	1.00	84.8

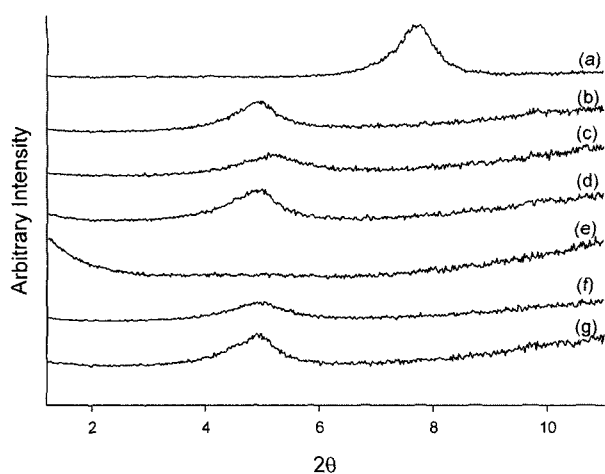


Figure 1. XRD patterns of (a) Na-MMT, (b) MAI/Na-MMT nanocomposite, (c) C03E0, (d) C03E06, (e) C03E06W (polymerized powder), (f) C10E20W, and (g) C03E06W (after pressing).

increased from 11.2 to 17.7 Å by the intercalation of MAI into the gallery of Na-MMT, similar to the case of previously reported PEO intercalated Na-MMT nanocomposites.^{17,18} The weight loss by pyrolysis in a furnace at 600 °C showed that the MAI intercalated in the gallery was 0.22 g/g-Na-MMT. This value was slightly less than 0.30 g/g-Na-MMT, which was previously reported as the maximum value to be intercalated in the case of PEO/Na-MMT nanocomposites.¹⁸

Figure 1(c)–(e) show the XRD patterns of PMMA/Na-MMT nanocomposites. The XRD patterns of Series I had a peak at $2\theta = 5.2^\circ$. Typical example is that of C03E0 shown in Figure 1(c). This shows that the gallery gap of Na-MMT was expanded to 17.0 Å by the intercalated PMMA molecules. C03E06 (Figure 1(d)) and other Series II samples had a peak at $2\theta = 5.0^\circ$. This peak position was the same as that of MAI/Na-MMT nanocomposite (Figure 1(b)), which suggested that the segment intercalated between the galleries of Na-MMT might be the PEG segment originated from MAI. In contrast, C03E06W (Figure 1(e)) did not have any distinct peak at angles above $2\theta = 2^\circ$. This showed that ordered face-face layer morphology of Na-MMT was scattered. However, a weak peak at $2\theta = 4.9^\circ$ developed as the content of Na-MMT was increased as can be seen in Figure 1(f), which shows that some silicate layers aggregated and ordered intercalated structures developed partially. When the polymerized powder of Series III was melt pressed at 140 °C, a peak at $2\theta = 5.0^\circ$ appeared as shown in Figure 1(g). This peak position was the same as those of MAI/Na-MMT nanocomposite of Figure 1(b) and Series II. These results suggested that silicate layers rearranged into intercalated structures by melt pressing and that the segment intercalated between the galleries of Na-MMT might mainly be the PEG segment. We observed that this change in the XRD pattern was not evident when the samples of Series III were annealed at 250 °C in DSC up to 1 hr without any external force. This showed the external force enhanced the rear-

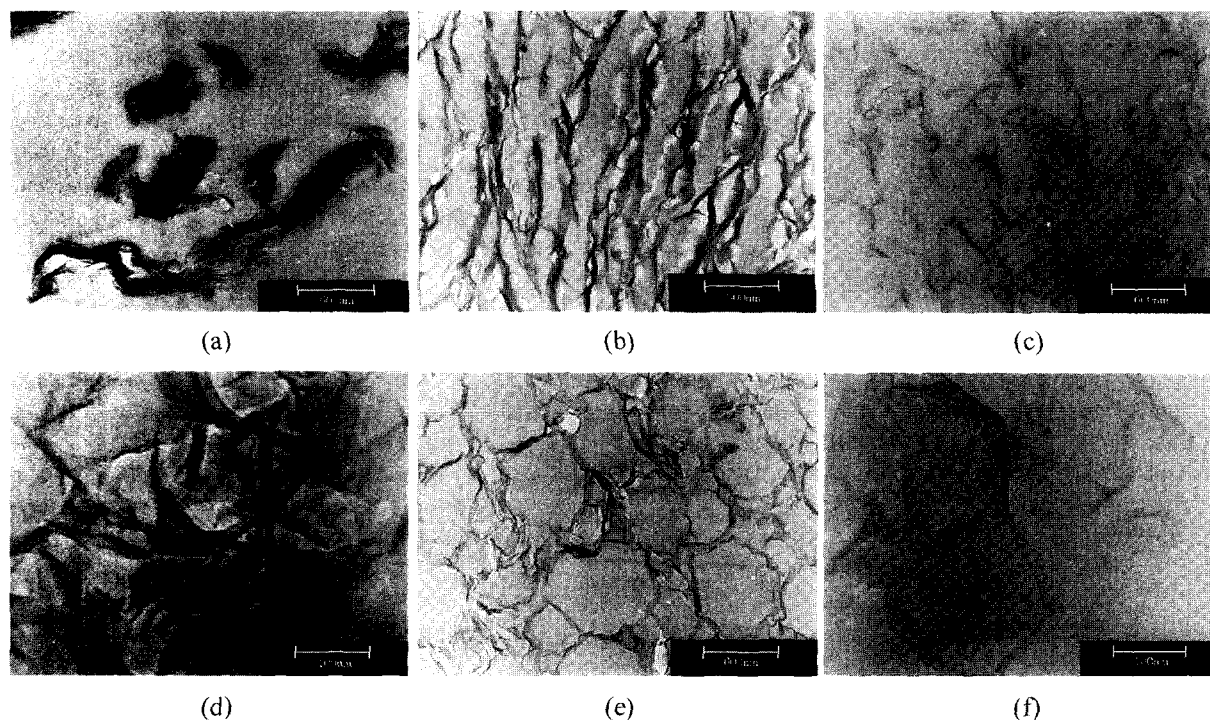


Figure 2. TEM micrographs of PMMA/Na-MMT nanocomposites : (a) C03E0; (b) C03E06; (c) and (d) C03E06W; (e) and (f) C05E10W.

rangement of silicate layers.

The morphology of the PMMA/Na-MMT nanocomposite observed by TEM is shown in Figure 2 to support the results of the XRD. Figure 2(b) shows that the dispersion of Na-MMT was enhanced by the PEG segment which originated from MAI and was linked to the PMMA segment when compared with Figure 2(a), which showed typical immiscible nanocomposite morphology with unevenly dispersed large aggregates of Na-MMT.²⁴⁻²⁶ Figure 2(c) shows that a much better clay dispersion with substantial curvature was obtained by polymerization after water swelling of the MAI intercalated Na-MMT. Although the dispersion of Na-MMT shown in Figure 2(c) is not so homogeneous as in Nylon-6/organoclay nanocomposite,²⁶ it was not easy to observe any ordered face-face layer morphology, generally observed with nanocomposites having intercalated morphology, even at high magnification. Instead, as can be seen in Figure 2(d), the morphologies of silicate layers which were largely distorted with substantial curvature were observed at Na-MMT-rich regions. This shows that the silicate layers, which were delaminated by intergallery polymerization, agglomerated again because the homogeneous dispersion of delaminated hydrophilic silicate layers in the hydrophobic PMMA matrix was not thermodynamically stable. However, the results of XRD (Figure 1(e)) and TEM (Figure 2(d)) suggest that ordered face-face layer morphology was not developed easily. In Figure 2(e), we can see that honeycomb-like structure was developed by agglomeration at higher content of Na-MMT. Although the morphology of C05E10W also did not show distinct ordered face-face layer morphology of Na-MMT, even at high magnification as can be seen in Figure 2(f), the result of XRD (Figure 1(f)) suggests that some ordered parallel structure of silicate layers were developed during reagglomeration at a higher content of Na-MMT.

The exfoliated nanocomposites systems can do fall into three categories, homogeneously exfoliated, heterogeneously exfoliated, and intercalated/exfoliated.²⁶ According to this classification, we think that C03E06W (Figure 1(e) and Figure 2(c) and (d)) has mainly the morphology of heterogeneously exfoliated and that C03E10W (Figure 1(f) and Figure 2(e) and (f)) has that of intercalated/exfoliated, respectively.

It was reported that thermal decomposition resistance was enhanced in the presence of clay by the thermal insulation effect of clay.^{13,21} The increase of thermal decomposition temperature by clay may also be associated with barrier property of silicate layers having high aspect ratio that hinders diffusion of the volatile decomposition products.^{13,27} To examine this effect, thermogravimetric analysis was carried out with the polymerized PMMA/Na-MMT nanocomposite powder. The temperature, where 10% weight loss occurred, is given in Table II. Table II shows that the efficiency of the enhancement of thermal degradation resistance by dispersed

Table II. Thermal Properties of PMMA/Na-MMT Nanocomposites

Sample	Temperature for 10 wt% Loss (°C)	T_g (°C)	
		Polymerized Powder	Melt Pressed
<i>Series I</i>			
C00E0	233	97	104
C03E0	242	120	107
C05E0	274	112	107
C07E0	268	112	101
<i>Series II</i>			
C03E06	276	120	103
C05E10	287	114	105
C07E14	297	116	107
<i>Series III</i>			
C03E06W	315	126	110
C05E10W	326	127	117
C07E14W	334	128	118
C10E20W	334	132	123

Na-MMT was elevated by improved dispersion according to the order, Series I < Series II < Series III. Series III shows about a 80~100 °C increase of the decomposition temperature for 10% weight loss compared to pristine PMMA.

In the nanocomposites, the T_g of matrix polymer increases compared with pristine polymer, because the segmental motions of the polymer chains are restricted at the organic-inorganic interface, due to the confinement of polymer chains between the silicate layers, as well as the silicate surface-polymer interaction in the nanostructured composites.^{28,29} The T_g 's of PMMA/Na-MMT nanocomposites measured by DSC are shown in Table II. The PMMA/Na-MMT nanocomposites generally had higher T_g compared to that of pristine PMMA, 97 °C, which showed that the chain mobility of PMMA was reduced by interaction with silicate layers. Table II also shows that the T_g of polymerized nanocomposite powder decreased after melt pressing.

The agglomeration of silicate layers, which we observed by XRD pattern change shown in Figure 1(e) and 1(g), by external force during melt compression seemed to have been a cause of this T_g decrease. The nanocomposites of Series III showed distinct T_g elevation which increased with the content of Na-MMT. However, this variation of T_g due to Na-MMT content was not as evident in the nanocomposites of Series I and Series II. These results showed that Na-MMT was more homogeneously dispersed in the PMMA matrix in Series III compared to that in Series I or Series II. The increase of T_g , about 30 °C observed in the nanocomposite powders of Series III were significantly higher than

previously reported values for exfoliated PMMA/Na-MMT nanocomposites, which were less than 15 °C.^{13,21} This supported the conclusion that our method was effective for the exfoliation of Na-MMT in a PMMA matrix.

Conclusions

Our experimental results show that MAI intercalated between the lamellae of Na-MMT effectively initiated the intergallery polymerization of MMA. The distinct increases of thermal degradation temperatures and T_g support the effectiveness of this method. Our experience that polymerization does not proceed by intercalated MAI without water-swelling shows that water helps the diffusion of MMA into the hydrophilic gallery where the initiator exists. Our results also show that the PEG segment linked to the PMMA segment enhances the compatibility between hydrophilic Na-MMT and hydrophobic PMMA. However, the PEG segment seems to enhance morphology change from an exfoliated to an intercalated structure by melt-pressing because the structure that the PEG segment is intercalated in Na-MMT has a high stability.

Acknowledgements. This work was supported by University of Ulsan Research Fund of 2003.

References

- (1) P. C. Le Baron, Z. Wang, and T. J. Pinnavaia, *Appl. Clay Sci.*, **15**, 11 (1999).
- (2) E. P. Giannelis, *Appl. Organometal. Chem.*, **12**, 675 (1998)
- (3) T. J. Pinnavaia and G. W. Beall, Eds., *Polymer-Clay Nanocomposites*, John Wiley & Sons, Chichester, 2000.
- (4) J. W. Gilman, C. L. Jackson, A. B. Morgan, R. Harris, Jr., E. Manias, E. P. Giannelis, M. Wuthenow, D. Hilton, and S. H. Phillips, *Chem. Mater.*, **12**, 1866 (2000).
- (5) H. Ishida, S. Campbell, and J. Blackwell, *Chem. Mater.*, **12**, 1260 (2000).
- (6) Y. Kojima, A. Usuki, M. Kawasumi, A. Okada, T. Kurauchi, and O. Kamigaito, *J. Polym. Sci., Polym. Chem.*, **31**, 983 (1993).
- (7) T. Lan and T. J. Pinnavaia, *Chem. Mater.*, **6**, 2216 (1994).
- (8) Y. I. Tien and K. H. Wei, *Macromolecules*, **34**, 9045 (2001).
- (9) M. Xu, Y. S. Choi, K. H. Wang, J. H. Kim, and I. J. Chung, *Macromol. Res.*, **11**, 410 (2003).
- (10) J. G. Ryu, J. W. Lee, and H. Kim, *Macromol. Res.*, **10**, 187 (2002).
- (11) M. B. Ko, M. Park, J. Kim, and C. R. Choe, *Korea Polym. J.*, **8**, 95 (2000).
- (12) M. B. Ko, S. Lim, J. Kim, C. R. Choe, M. S. Lee, and M. G. Ha, *Korea Polym. J.*, **7**, 310 (1999).
- (13) X. Huang and W. J. Brittain, *Macromolecules*, **34**, 3255 (2001).
- (14) M. C. Weimer, H. Chen, E. P. Giannelis, and D. Y. Sogah, *J. Am. Chem. Soc.*, **121**, 1615 (1999).
- (15) Q. Zhou, X. Fan, C. Xia, J. Mays, and R. Advincula, *Chem. Mater.*, **13**, 2465 (2001).
- (16) H. Böttcher, M. L. Hallensleben, S. Nuß, H. Wurm, J. Bauer, and P. Behrens, *J. Mater. Chem.*, **12**, 1351 (2002).
- (17) P. Aranda and E. Ruiz-Hitzky, *Chem. Mater.*, **4**, 1395 (1992).
- (18) J. Wu and M. M. Lerner, *Chem. Mater.*, **5**, 835 (1993).
- (19) M. Okamoto, S. Morita, H. Taguchi, Y. H. Kim, T. Kotaka, and H. Tateyama, *Polymer*, **41**, 3887 (2000).
- (20) C. Zeng and L. J. Lee, *Macromolecules*, **34**, 4098 (2001).
- (21) Y. S. Choi, M. H. Choi, K. H. Wang, S. O. Kim, Y. K. Kim, and I. J. Chung, *Macromolecules*, **34**, 8978 (2001).
- (22) A. Ueda and S. Nagai, *J. Polym. Sci., Polym. Chem.*, **24**, 405 (1986).
- (23) M. M. Al-Esaimi, *J. Appl. Polym. Sci.*, **64**, 367 (1997).
- (24) B. Liao, H. Liang, and Y. Pang, *Polymer*, **42**, 10007 (2001).
- (25) H. R. Fisher, L. H. Gielgens, and T. P. M. Koster, *Acta Polym.*, **50**, 122 (1999).
- (26) A. B. Morgan and J. W. Gilman, *J. Appl. Polym. Sci.*, **87**, 1329 (2003).
- (27) J. G. Doh and I. Cho, *Polym. Bull.*, **41**, 511 (1998).
- (28) P. Uthirakumar, K. S. Nahm, Y. B. Hahn, and Y. S. Lee, *Eur. Polym. J.*, **40**, 2437 (2004).
- (29) M. W. Noh and D. C. Lee, *Polym. Bull.*, **42**, 619 (1999).